

# We are IntechOpen, the world's leading publisher of Open Access books Built by scientists, for scientists

6,900

Open access books available

185,000

International authors and editors

200M

Downloads

Our authors are among the

154

Countries delivered to

TOP 1%

most cited scientists

12.2%

Contributors from top 500 universities



WEB OF SCIENCE™

Selection of our books indexed in the Book Citation Index  
in Web of Science™ Core Collection (BKCI)

Interested in publishing with us?  
Contact [book.department@intechopen.com](mailto:book.department@intechopen.com)

Numbers displayed above are based on latest data collected.  
For more information visit [www.intechopen.com](http://www.intechopen.com)



# Optimal Design of Haptic Interfaces

Volkan Patoglu and Aykut Cihan Satici  
Sabanci University  
Istanbul, Turkey

IntechOpen

## 1. Introduction

*Haptic interfaces* are computer-controlled motorized devices that physically interact with human operators to render presence of computationally mediated environments. Ideal haptic devices are desired to withstand human applied forces with very high stiffness and be capable of displaying a full range of impedances down to the minimum value humans can perceive. The performance of a haptic interface under closed loop control is measured by the *transparency* of the display, that is, by quantifying the correspondence between the desired and actually rendered impedance values. During haptic rendering, the haptic interface is coupled to the control system and its existence results in parasitic effects on the displayed impedances, deteriorating the perfect transparency. Therefore, independent of the control algorithm, both the kinematic and dynamic performance of the haptic device have an impact on the overall performance of the haptic display.

Robotic manipulators with parallel kinematic chains are popular among haptic interfaces due to their inherent advantages in satisfying requirements of haptic applications with respect to their serial counterparts. Parallel mechanisms offer compact designs with high stiffness and have low effective inertia since their actuators can be grounded in many cases. In terms of dynamic performance, high position and force bandwidths are achievable with parallel mechanisms thanks to their light, but stiff structure. Besides, parallel mechanisms do not superimpose position errors at joints; hence, can achieve high precision.

Despite these favorable characteristics of parallel mechanisms, optimal design of such mechanisms with closed kinematic chains is significantly more challenging. Parallel mechanisms have smaller workspace with possible singularities within the workspace and their kinematic, dynamic, and singularity analysis are considerably harder than that of serial manipulators. Due to the additional complexities involved, the dimensional synthesis of parallel mechanisms is still an active area of research.

Optimum design of parallel mechanisms, even for a single objective function, is challenging due to the nonlinear, large scale nature of such mechanisms (Lee & Kim, 2006) and non-convex properties of performance indices with respect to the design variables (Qi & Womersley, 1996). Many different optimization approaches applicable to nonlinear, non-convex optimization problems such as genetic algorithms (Lee et al., 2001; Lee & Kim, 2006; Stuckman & Easom, 1992; Zheng & Lewis, 1994), simulated annealing (Risoli et al., 1999), Bayesian techniques (Stuckman & Easom, 1992; Stuckman et al., 1991), Monte-Carlo simulations (Stuckman & Easom, 1992; Zheng & Lewis, 1994), controlled randomized searches (Lou et al., 2008), performance charts (Liu & Wang, 2007), workspace atlases (Liu et al., 2006), and branch and

bound methods (Stocco et al., 1998) have been applied to design optimization of parallel mechanisms. In general, deterministic methods can get stuck at a local optimum, heuristic methods cannot guarantee optimality of the converged solution, while branch and bound type methods are only as accurate as the discretization selected.

While designing the geometry of a haptic interface, various performance criteria such as kinematic and dynamic isotropy, singularity-free workspace, sensitivity, and transmission capability have to be considered *simultaneously*. The performance with respect to any of these criteria cannot be improved without deteriorating another; hence, design trade-offs are inevitable. Determination of optimal dimensions with respect to many design criteria is a difficult problem and should be handled with multi-objective optimization methods so that trade-offs can be assigned in a systematic manner.

As emphasized earlier, an optimal design of a haptic interface can only be achieved by considering many competing objectives. There exists several studies in which multiple design criteria have been addressed for this purpose. The studies that can be categorized under *scalarization methods* address the multi-criteria optimization problem in an indirect manner, by first transforming it into a (or a series of) single objective (scalar) problem(s). Among these approaches, Hayward *et al.* define the relationship between multiple criteria and utilize sensitivities of these criteria to conduct a hierarchical optimization study (Hayward et al., 1994). Multiple objectives are considered sequentially in (Alici & Shirinzadeh, 2004; Krefft et al., 2005; Risoli et al., 1999; Stocco et al., 1998) by searching for parameter sets resulting in near optimal kinematic performance and then selecting the design exhibiting the best dynamic performance from this reduced parameter space. Task-priority (Chen et al., 1995), probabilistic weighting (McGhee et al., 1994), composite index (Lee et al., 2001), and tabular methods (Yoon & Ryu, 2001) are among the other scalarization approaches that consider multiple criteria. Scalarization methods possess the inherent disadvantage of their aggregate objective functions requiring preferences or weights to be determined *a priori*, *i.e.* before the results of the optimization process are actually known (de Weck, 2004). Since assigning proper weights or prioritizing different criteria is a problem dependent, non-trivial task, these techniques fall short of providing a general framework to the design of the parallel mechanisms.

The alternative approach is classified as *pareto methods*, which incorporate all optimization criteria within the optimization process and address them simultaneously to find a set of non-dominated designs in the objective space. Pareto methods allow the designer to make an informed decision by studying a wide range of options, since they contain solutions that are optimum from an *overall* standpoint; unlike scalarization techniques that may ignore this trade-off viewpoint. In literature Krefft *et al.* applied a modified genetic algorithm (GA) based Pareto method to design parallel mechanisms (Krefft & Hesselbach, 2005a; Krefft et al., 2005). Similarly, in (Stan et al., 2006) GA is applied to multi criteria optimization of a 2-DoF parallel robot. Finally, in (Unal et al., 2008a;b) authors proposed a multi-objective design framework for optimization of parallel mechanisms based on Normal Boundary Intersection (NBI) method (Das & Dennis, 1996). The proposed framework has been applied to design of rehabilitation robots (Erdogan et al., 2009; Unal & Patoglu, 2008b), robotic exoskeletons (Satici et al., 2009; Unal & Patoglu, 2008a), and compliant micro mechanisms (Tokatli & Patoglu, 2009). This framework is computational efficient, applicable to other performance indices, and easily extendable to include further design criteria that may be required by the application.

In this chapter, the multi-objective design framework for optimization of parallel mechanisms, first proposed by the authors in (Unal et al., 2008a;b) is reviewed. Global kinematic and dynamic performance of parallel mechanisms defined over a pre-specified singularity free workspace are maximized simultaneously and the Pareto-front curve for these two criteria is obtained. Firstly, the global optima of non-convex min-max performance criteria are solved independently from each other, using a modified branch and bound algorithm, called culling algorithm (Stocco et al., 1998). Once optimal solutions of each single criteria optimization problem are obtained, Normal Boundary Intersection (NBI) method (Das & Dennis, 1996), which performs a deterministic geometric search within the objective space, is utilized to efficiently compute uniformly distributed design solutions on the Pareto-front curve.

The chapter is organized as follows: Section 2 identifies and categorizes relevant design objectives for haptic interfaces. Section 3 introduces the sample mechanism used for the analysis, a 3-degrees of freedom (DoF) Modified Delta Mechanism. Section 4 formulates the optimization problems, while Section 5 explains the optimization methods used to address the single and multi-criteria optimization problems. Section 6 presents and discusses the results of the optimization problems. Finally, Section 7 concludes the chapter.

## 2. Design Objectives

Following the terminology of Merlet (Merlet, 2006), one can categorize the performance requirements of a mechanism into four distinct groups: *Imperative* requirements that must be satisfied for any design solution, *optimal* requirements for which an extremal value of the index is required, *primary* requirements which take place in the specifications but can be modified to some extent to ensure a design solution, and *secondary* requirements which do not appear in the specifications but can be utilized to choose between multiple design solutions. Ensuring the safety and complying with the ergonomic needs of the human operator are two imperative design requirements every haptic interface must satisfy. Safety is typically assured by the selection of back-drivable actuation and power transmission<sup>1</sup> with force/torque limits implemented in software, while predetermined ergonomic workspace volumes are imposed at the kinematic synthesis level. The absence of singularities in the workspace is another imperative design requirement that ensures the forward and inverse kinematics of the robot be solved uniquely at each point within the workspace.

Both kinematic and dynamic performance of parallel mechanisms are to be optimized to achieve haptic devices with low parasitic effects. Specifically, to achieve high force bandwidths and a uniform "feel" for the device, kinematic/dynamic isotropy and stiffness of the device have to be maximized while its apparent inertia is being minimized. To quantify performance, several design matrices, including Jacobian and inertia matrices, are studied and to date many scalar performance indices have been proposed. These indices either quantify the directional independence (uniformity) of configuration dependent design matrices or represent a distance to a singular configuration. Since singular values of a matrix provide a versatile metric to quantify its properties, most of the indices are derived as a function of these values. These performance metrics are further discussed in the next subsection.

A common primary requirement for haptic interfaces is the workspace volume index (Merlet, 2006), the ratio between the workspace volume and the volume of the robot. Even though predetermined workspace volumes are generally imposed as imperative requirements, a large

---

<sup>1</sup> In this chapter, we limit our discussion to impedance type devices due to their widespread use, even though admittance type devices can also be treated using an analogous framework.

workspace volume index is still desired to reduce the collisions of the device with the operator or the environment. The footprint area is yet another primary requirement commonly imposed during design.

Finally, the secondary requirements include low backlash, low-friction, high back-drivability, and low manufacturing costs. Friction, backlash, and back-drivability are mainly influenced by the selection of the actuators and the transmission, while choice of link lengths may have an influence on manufacturing costs.

## 2.1 Measuring Kinematic and Dynamic Performance

To measure kinematic performance, properties of the Jacobian matrix ( $J$ ) are studied. Condition number, proposed by Salisbury and Craig (Salisbury & Craig, 1982), describing the worst-case behavior at a given configuration is one of the most commonly used kinematic performance measures. Given as the ratio of the minimum and maximum singular values of the Jacobian matrix, this measure locally characterizes directional isotropy for both force/motion transmission accuracy and actuator utilization of a manipulator. Another popular index, manipulability, measures the ease of arbitrarily changing the position and orientation of the end effector and is calculated by taking the product of singular values of the Jacobian matrix (Yoshikawa, 1985b). Sensitivity characterizes the precision of a manipulator by measuring the change in end-effector configuration with respect to small perturbations of joint angles and is given by the sum of the absolute values of the Jacobian matrix elements in a single row (Grace & Colgate, 1993). Finally, minimum singular value of the Jacobian matrix is also proposed as a kinematic performance measure (Klein & Blaho, 1987) quantifying the skewness of the velocity response.

All of the mentioned indices are *local* measures of kinematic performance; therefore, are not constant over the entire workspace. Extensions of these indices have been proposed to characterize the performance of a manipulator over the entire workspace. Gosselin and Angeles proposed *global* condition indices based on the integral of local kinematic performance measures over the workspace (Gosselin & Angeles, 1991). However, being average values, these indices fail to capture possible low performance configurations (near singular points) within the workspace. Moreover, integrating a local measure can be computationally expensive. Mean of the minimum singular value has also been proposed as global measure in order to characterize the path velocity of parallel robots (Krefft & Hesselbach, 2005b). Since mean values are not sufficient to guarantee homogeneity of performance, standard deviation of the minimum singular value has also been introduced as a measure (Krefft & Hesselbach, 2005b). Other global indices include global payload index that measures the force transmission capability (Ozaki et al., 1996). Finally, the global isotropy index ( $GII$ ), introduced in (Stocco et al., 1998) by Stocco *et al.*, is a workspace inclusive worst-case kinematic performance measure that is intolerant of poor performance over the entire workspace.  $GII$  is calculated as the ratio of the minimum of the smallest singular value and the maximum of the largest singular value of the Jacobian matrix over the workspace.

In this chapter, a global performance index is chosen to quantify the kinematic isotropy of haptic interfaces since the objective of the design problem is to minimize the parasitic effects of the manipulator over the workspace. Even though any global index can be utilized within the framework presented, the conservative workspace inclusive worst-case performance measure that is intolerant of poor performance over the entire workspace,  $GII$ , is preferred. As a global worst case performance measure, maximizing  $GII$  corresponds to designing a mechanism with best worst-case kinematic performance. Moreover, an optimal  $GII$  results in a uniform

Jacobian matrix, while also increasing the efficiency of utilization of the actuators.  $\mathcal{GII}$  can be mathematically expressed as

$$\mathcal{GII} = \min_{\gamma_0, \gamma_1 \in W} \frac{\underline{\sigma}(J(\alpha, \gamma_0))}{\bar{\sigma}(J(\alpha, \gamma_1))} \quad (1)$$

where  $J$  represents the Jacobian of the manipulator,  $\underline{\sigma}$  and  $\bar{\sigma}$  are the minimum and maximum singular values of the Jacobian matrix,  $\gamma_0$  and  $\gamma_1$  are the configurations in the workspace that result in the extreme singular values,  $\alpha$  is the column matrix of design variables, and  $W$  represents the workspace.

Dynamic performance is measured in a similar manner to the kinematic performance, but properties of the inertia matrix ( $M$ ) capturing the relation between actuator force/torque and end-effector acceleration, are studied. The goal for improving dynamic performance is to minimize inertial effects that conflict with high acceleration demands. To characterize *local* dynamic performance Asada defined the effective inertia matrix expressing the homogeneity of the moment of inertia of the non-redundant manipulators and introduced the concept of generalized inertia ellipsoid (Asada, 1983). Yoshikawa proposed a dynamic manipulability measure (Yoshikawa, 1985a), which is an extension of manipulability concept and measures the degree of arbitrariness in changing end-effector accelerations. Dynamic manipulability is calculated as the product of singular values of  $M^{-1}$  matrix. Angeles *et al.* defined the dynamical conditioning index which measures dynamical coupling and numerical stability of the generalized inertia matrix of manipulators (Ma & Angeles, 1990). Finally, swiftness, a measure to characterize the attitude of the manipulator to produce high end-effector accelerations, is proposed by Di Gregorio *et al.* which can also be applied to planar manipulators with non-homogeneous generalized coordinates (Gregorio & Parenti-Castelli, 2005).

Similar to the case of local kinematic performance indices, extensions to local dynamic indices have been proposed to characterize the performance of a manipulator over the entire workspace. Calculating the mean value and standard deviation of the local dynamic indices are among the most commonly used approaches to achieve a global dynamic performance index. A global dynamic index ( $\mathcal{GDI}$ ) is introduced in (Stocco *et al.*, 1998) to quantify the global worst-case performance of a manipulator.  $\mathcal{GDI}$  measures the largest effect of mass on the dynamic performance by calculating the maximum largest singular value over the workspace of the effective mass matrix at the end-effector and is computed as the inverse of the maximum of the largest singular value.

To be consistent with the metric chosen for the kinematic performance, the workspace inclusive best worst-case performance measure ( $\mathcal{GDI}$ ) is used to quantify dynamic performance. As mentioned earlier, any dynamic index could be utilized in the framework introduced, but this decision is conservative and intolerant of poor performance over the entire workspace. As a global worst-case performance measure, maximizing  $\mathcal{GDI}$  results in reduced maximum largest singular value of the effective mass matrix, decreasing the inertial interference by the system.  $\mathcal{GDI}$  can be mathematically expressed as

$$\mathcal{GDI} = \min_{\gamma \in W} \frac{1}{1 + \bar{\sigma}(M(\alpha, \beta, \gamma))} \quad (2)$$

where  $M$  represents effective inertia matrix of the manipulator as seen at the end effector,  $\bar{\sigma}$  is the maximum singular value of the effective inertia matrix,  $\gamma$  is the configuration in the workspace that results in the maximum singular value,  $\alpha$  is the column matrix of design variables, and  $W$  represents the workspace.

In general, since entries of the Jacobian and the inertia matrices may not be homogenous in units, proper normalization is necessary such that the measures defined on these matrices are meaningful. Among several approaches proposed in literature, normalization with a characteristic length (Khan & Angeles, 2006; Krefft & Hesselbach, 2005b) or a nominal link length (Lee et al., 2001), and partitioning the matrices into translational and rotational parts (Krefft & Hesselbach, 2005b; Lee & Kim, 2006) are the most popular choices. Normalization is not necessary for the sample problem presented in this chapter, as it possesses only a translational workspace.

### 3. Modified Delta Mechanism

The optimization framework reviewed in this chapter is demonstrated over a spatial 3-DoF Modified Delta parallel mechanism (see Figure 1). The method discussed in this chapter constitutes a general framework for optimal dimensional synthesis of mechanisms and is by no means limited to the sample mechanism studied.

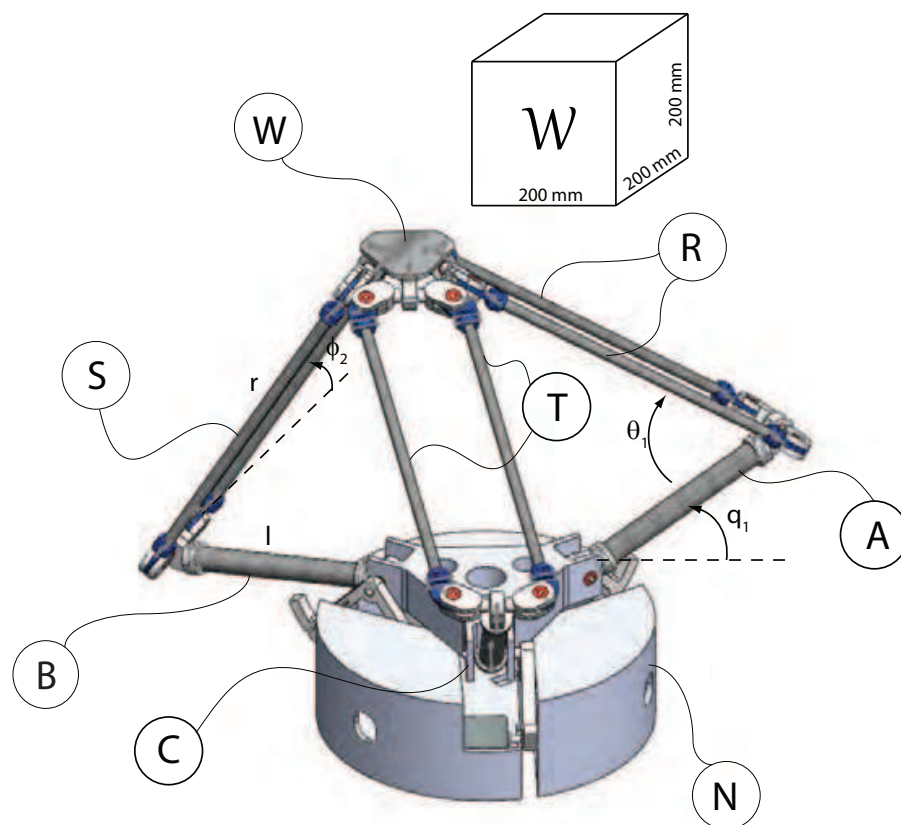


Fig. 1. The Modified Delta Mechanism

The Modified Delta Mechanism, first introduced by Clavel (Clavel, 1988), and further analyzed in (Pierrot et al., 1990), consists of eight bodies: a base platform  $N$ , three lower links  $A$ ,  $B$ ,  $C$ , three upper links  $R$ ,  $S$ ,  $T$ , and a moving platform  $W$ . The end-effector held by the operator is rigidly attached to the moving platform  $W$ . The three lower links are connected to the base platform via revolute joints whose axes of rotation are oriented along the tangents of  $N$ .

The upper three links are coupled to the lower links via revolute joints. Each of them is a planar four-bar parallelogram, which can perform one DoF motion constrained in its plane. The moving platform is connected to these three upper links by means of revolute joints whose axes of rotation are again oriented along the tangents of  $W$ . In this chapter, the analysis is limited to a symmetric modified delta mechanism where the revolute joints at the base and at the moving platform are spaced at  $120^\circ$  along the circumference of each platform whose radii ratio is 0.5. Moreover, the lengths of each of the lower links and similarly that of each of the upper links are considered to be the same. The modified delta mechanism has three translational DoF ( $x, y, z$ ) of the moving platform  $W$  with respect to the Newtonian reference frame  $N$ . The controlled DoF are the three revolute joints, with which the lower three links are connected. Kinematic and dynamic models of the Modified Delta mechanism are further detailed in (Li & Xu, 2005; Pierrot et al., 1990; Tsai et al., 1996).

A modified delta mechanism can be characterized by lengths  $l$  and  $r$  of its two links, since the rest of the mechanism is designed to be symmetric. To quantify the orientation of each link, joint angles  $q_i, \theta_i, \phi_i, (i = 1..3)$ , are introduced. The workspace of the mechanism is selected to be a cube of length 200mm, and is placed at a fixed location in global coordinate frame:  $[x, y, z]^T = [0 - 200, 0 - 200, 200 - 400]^T$  mm as presented in Figure 1. Table 1 presents the design variables  $\alpha$  and design parameters  $\beta$  (parameters that do not change during the design process) for the modified delta mechanism.

	Symbol	Definition	Unit
$\alpha_1$	$l$	Length of the lower links	mm
$\alpha_2$	$r$	Length of the upper links	mm
$\beta_1$	$x = 0 - 200$	Workspace along $x$ -direction	mm
$\beta_2$	$y = 0 - 200$	Workspace along $y$ -direction	mm
$\beta_3$	$z = 200 - 400$	Workspace along $z$ -direction	mm

Table 1. Design variables  $\alpha$  and parameters  $\beta$  for the Modified Delta Mechanism

#### 4. Optimization Problem

As discussed in Section 2, two objective functions characterizing the kinematic and dynamic performances of the mechanism are considered in this chapter. The objective of optimization is to maximize the worst kinematic isotropy of the mechanism ( $GII$ ) while simultaneously minimizing the effective mass (maximum singular value of the effective mass matrix or  $GDI$ ). In this study, it is assumed that the inertia of the mechanism is only due to those of each link; thus, other inertial factors such as inertia of the actuators etc. are neglected. The negative null form of the multi-objective optimization problem can be stated as

$$\begin{aligned} \max \mathbf{F}(\alpha, \beta, \gamma) \\ \mathbf{G}(\alpha, \beta) \leq 0 \\ \alpha_l < \alpha < \alpha_u \end{aligned} \quad (3)$$

where  $\mathbf{F}$  represents the column matrix of objective functions that depend on the design variables  $\alpha$ , parameters  $\beta$ , and workspace positions  $\gamma$ . Symbol  $\mathbf{G}$  represents the inequality constraint function that also depends on design variables and parameters. Finally,  $\alpha_l$  and  $\alpha_u$  correspond to the lower and upper bounds of the design variables, respectively.

For the modified delta mechanism, the column matrix  $\mathbf{F}$  is simply given as

$$\mathbf{F} = \begin{bmatrix} \mathcal{GDI} \\ \mathcal{GII} \end{bmatrix} \quad (4)$$

The constraints on the other hand, are implicitly imposed during the kinematic analysis of the parallel mechanism, which is carried out using numerical integration.

## 5. Methods

In the previous section, the formulation for the multi-criteria optimization problem for best worst-case performance of a haptic interface is described. Before addressing the multi-criteria optimization problem, the nature of the problem with respect to the selected performance criteria is to be studied. Inspecting the performance criteria, one can conclude that both  $\mathcal{GII}$  and  $\mathcal{GDI}$  are non-convex with respect to the design variables. Moreover, as workspace inclusive measures, their calculation requires searches over the workspace. As discussed in the introduction, several methods have been proposed to solve for the single criteria optimization problem of parallel manipulators. In general, descent methods suffer from getting trapped at local optima while heuristic methods cannot guarantee optimality of their solution. Feasibility and efficiency of a branch-and-bound type method, called *culling algorithm*, is advocated in the literature to address single objective min-max problems (Stocco et al., 1998).

In this chapter, a modified version of the culling algorithm is used to independently solve for the optimum designs with respect to  $\mathcal{GII}$  and  $\mathcal{GDI}$ . The culling algorithm improves the computational efficiency of a brute-force method by reducing (culling) the amount of searches required through effective performance comparisons. The algorithm capitalizes on the fact that as a worst-case measure, once the global performance index for certain reference parameters is calculated conducting a search over the entire workspace, reduction of the feasible parameter set can be performed without performing any other searches over the workspace. Specifically, after a global index value is calculated for the reference parameters, comparisons with local indices at *only* a single configuration in the workspace. Hence, searches over workspace is significantly reduced as they are conducted only when it is necessary to calculate new reference global index values. Comparing all set of design variables to find the best worst-case index, the algorithm will converge to an optimum solution within the discretization accuracy. As the culling method substantially reduces the amount of workspace searches required by a brute-force method, it is a faster and more efficient algorithm to address min-max type problems.

Since the performance of the culling algorithm is highly dependent on the initial reference values assigned, a fast gradient-based optimization method, sequential quadratic programming (SQP), is used to solve for a local extrema that will serve as a good initialization value. This modification increases the efficiency of the algorithm by resulting in a higher culling rate at the first iteration. Once a solution is obtained, another SQP is invoked to converge to a guaranteed optima within the discretization region.

If the multi-criteria optimization problem is treated as multiple single objective problems where objective functions are handled independently, optimal solution for one criteria may result in an unacceptable design for the other. To achieve a “best” solution with respect to multiple criteria, the trade-off between objectives need to be quantified. Scalarization approaches assume apriori knowledge of this trade-off and convert the multi-criteria problem into a single objective one by assigning proper weights or priorities to each performance index. On the other hand, Pareto methods do not require any apriori knowledge about the design trade-offs and solve for the locus of all dominant solutions with respect to multiple objective functions, constituting the so-called the Pareto-front hyper-surface. Hence, designers

can make a more realistic choice between multiple “best” solutions and avoid the challenge of synthetically ranking their preferences.

There exists several methods to obtain the Pareto-front hyper-surface, among which Normal Boundary Intersection (NBI) method is one of the most featured. As the Pareto-front hyper-surface is a geometric entity in the objective space forming the boundary of the feasible region, NBI approach attacks the *geometric problem* directly by solving for single-objective constrained subproblems to obtain uniformly distributed points on the hyper-surface. NBI solves for subproblems which only depend on the defined optimization model, that is, chosen objective functions and design constraints since these equations map the feasible design space onto the attainable objective space. Given independent optimal solutions for each objective function (solutions of each single objective problem), called shadow points, NBI first constructs an hyper-plane in the objective space by connecting these shadow points with straight lines. Then, this hyper-plane is divided into grids that control the resolution of solutions on the Pareto-front hyper-surface. For each point on the grid, a geometric subproblem is solved to find the *furthest* point on the line that extends along the surface normal passing through the grid point and is in the feasible domain of the objective space. Hence, NBI obtains the Pareto-front by reducing the problem to many single-objective constrained subproblems. Number of subproblems can be adjusted by defining resolution of the grid that maps to the number of points on the Pareto-front hyper-surface. As the number of points increases, the computational time increases linearly, but since the method assumes spatial coherence and uses the solution of a subproblem to initialize the next subproblem, convergence time for each subproblem may decrease resulting in further computational efficiency.

NBI method results in exceptionally uniformly distributed points on the Pareto-front hyper-surface without requiring any tuning of the core algorithm. Moreover, once shadow points are obtained, NBI solves for the geometric problem directly utilizing a fast converging gradient-based method, evading the computationally demanding aggregate optimization problems required in most of the scalarization methods. Therefore, NBI method promises to be much faster and more efficient than other methods to obtain a well represented Pareto-front hyper-surface including aggregate methods such as weighted sums and evolutionary optimization approaches such as GA.

It should also be noted that the NBI method can solve for points on the non-convex regions of Pareto-front hyper-surfaces, a feature that is missing from the weighted sum methods. Compared to weighted sum techniques, NBI achieves higher solution efficiency as it does not suffer from clumping of solution in the objective space. NBI is also advantageous over other methods as it trivially extends to handle any number of objective functions. Compared to Multi-Objective Genetic Algorithm (MOGA) (Fonseca & Fleming, 1993) that requires problem dependent fitness and search related tuning and several steps to reach convergence, a standard NBI approach can map the Pareto-front hyper-surface with higher accuracy and uniformity, while also inheriting the efficiency of gradient-based methods.

Relying on gradient techniques, NBI assumes sufficient smoothness of the geometric problem at hand, but it has also been demonstrated that the method performs remarkably well even for non-smooth geometries (Rigoni & Poles, 2005). In the presence of non-continuous regions, multiple initializations of the NBI method may be required for efficiently generating the Pareto-front hyper-surface. For the case of strongly discontinuous geometries, hybridization with MOGA-II to supply feasible initialization points at each continuous sub-region can be employed, as proposed in (Rigoni & Poles, 2005). It is noted that since NBI relies on equality constraints, it is possible for NBI not to find a solution on the true Pareto-front hyper-surface,

converging to a local optima. In such a case, post processing on the solutions of NBI subproblems can be employed to filter out undesired dominated solutions.

## 6. Results and Discussion

Table 2 presents the results of the modified culling algorithm for the single objective problems, for best kinematic and dynamic isotropy, respectively. These results are obtained by conducting a global search over the entire parameter space with discretization step sizes of 0.5mm and 20mm for the parameter and workspace, respectively, and by performing several local searches with finer discretizations at the neighborhood of the results suggested by the global search.

	Best Design for Kinematic Isotropy	Best Design for Dynamic Isotropy	Unit
$GII$	0.36228	0.27348	–
$GDI$	0.18726	0.37294	–
$l$	484	300	mm
$r$	583	382	mm

Table 2. Results of independent optimizations with respect to  $GII$  and  $GDI$ .

Figure 2 presents the single objective surfaces plotted with respect to the design variables. While, subfigures 2(a) and 2(b) depict  $GII$  and  $GDI$  individually, in subfigures 2(c) and 2(d) functions are plotted on top of each other. In subfigure 2(c), both functions are supposed to be maximized, while in subfigure 2(d), a simple transformation is performed to revert the maximization into a minimization problem. As is evident from these figures, optimal values for each of these objective functions imply poor performance for the other objective function. Therefore, the trade-off curve has to be characterized, from which a sensible design choice can be made.

To characterize the trade-off between the single objective solutions, Pareto-front curve for the bi-objective optimization problem is constructed in Figure 3. Two different techniques are employed to form the Pareto-front curve, namely NBI method and aggregated performance index method. For the NBI method, a grid size of ten points is selected. In Figure 3 the distribution of points on the Pareto-front curve is marked by dots. For the second method, an aggregated performance index ( $API$ ) is defined as the weighted linear combination of  $GII$  and  $GDI$ . In particular,  $API = \lambda GII + (1 - \lambda) GDI$ , where  $0 \leq \lambda \leq 1$  denotes the weighting factor. Ten aggregated optimization problems are solved for ten equally spaced weighting factors utilizing the modified culling algorithm with discretization step sizes of 0.5mm for the parameter space and 20mm for the workspace. Circles in the Figure 3 denote the distribution of aggregate solutions on the Pareto-front curve and are marked with their corresponding weighting factor.

As expected, NBI method generates a very uniform distribution of points on the Pareto-front curve while the solutions of the aggregate problem are clumped at certain locations of the curve. To obtain a uniform distribution using the aggregated index approach, proper weights should be assigned. However, the characteristics of the weight distribution is not known before the problem is solved. Moreover, the aggregate performance index relies on the relatively costly culling algorithm to solve for each point on the Pareto-front curve and the accuracy of the solution is limited by the discretization step size chosen. In the Figure 3, the same solutions are obtained for different weighting factors, particularly for weighting factors  $\lambda = 0.1$  to

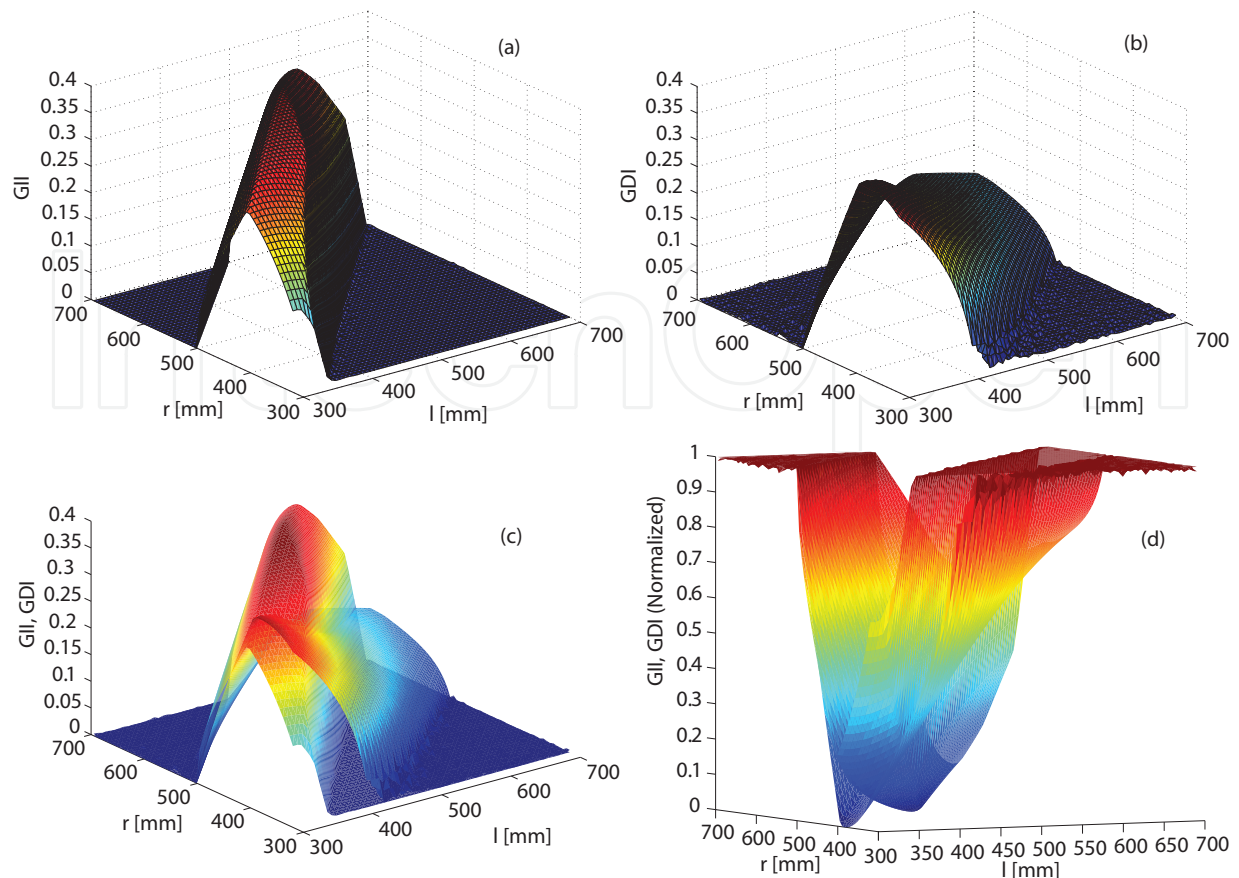


Fig. 2. Functions to be optimized depicted as surfaces. Subfigures (a) and (b) are GII and GDI respectively, while (c) and (d) represent both of them cast as minimization and maximization problems.

$\lambda = 0.3$ . Moreover, a large portion of the Pareto front is missed between  $\lambda = 0.7$  to  $\lambda = 0.8$ , due to the coarse discretization used. Unfortunately, solving for each aggregate performance index for all weighting factors is a computationally demanding task, limiting the density of discretization. NBI method possesses an inherent advantage in terms of computational cost, as it attacks the direct geometric problem to obtain the Pareto-front curve and utilizes continuous, computationally efficient gradient methods for the solution.

In addition to the efficiency offered via the uniform distribution of solutions on the Pareto-front curve, NBI approach results in *orders of magnitude* improvement in the computation time, especially for the design problem at hand, as depicted in Figure 4. All of the simulations presented in Figure 4 are performed using a 64 bit Windows XP workstation that is equipped with double Quad Core 3.20GHz 1600MHz Rated FSB Intel Xeon processors with 2x6MB L2 cache, and 8GB (4x2048) 800MHz DDR2 Quad Channel FBD RAM.

As can be observed from Figure 4, the aggregate problem scales geometrically with the discretization step size, rendering an accurate solution of even ten points on the Pareto-curve almost impossible for the simple sample problem at hand. On the other hand, NBI method with a  $10^{-8}$  tolerance solves for points on the Pareto-front curve very effectively, in about half the time of the weighted-sum approach with 2.5mm step size. Even though the accuracy of solutions obtained by the NBI method is dependent on the constraint tolerance set for the algorithm, convergence for NBI with all the tolerance values  $10^{-6}$  and  $10^{-8}$  are shown to be

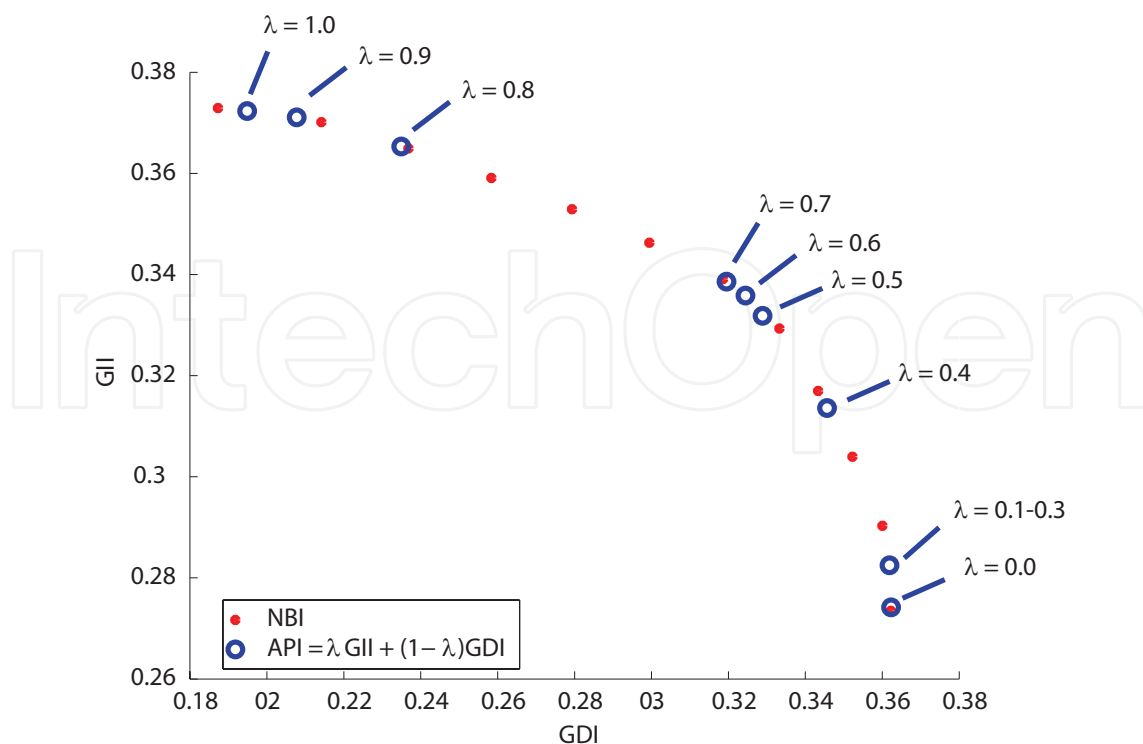


Fig. 3. Comparison of NBI and aggregated performance index methods. Symbol  $\lambda$  is the weighting factor.

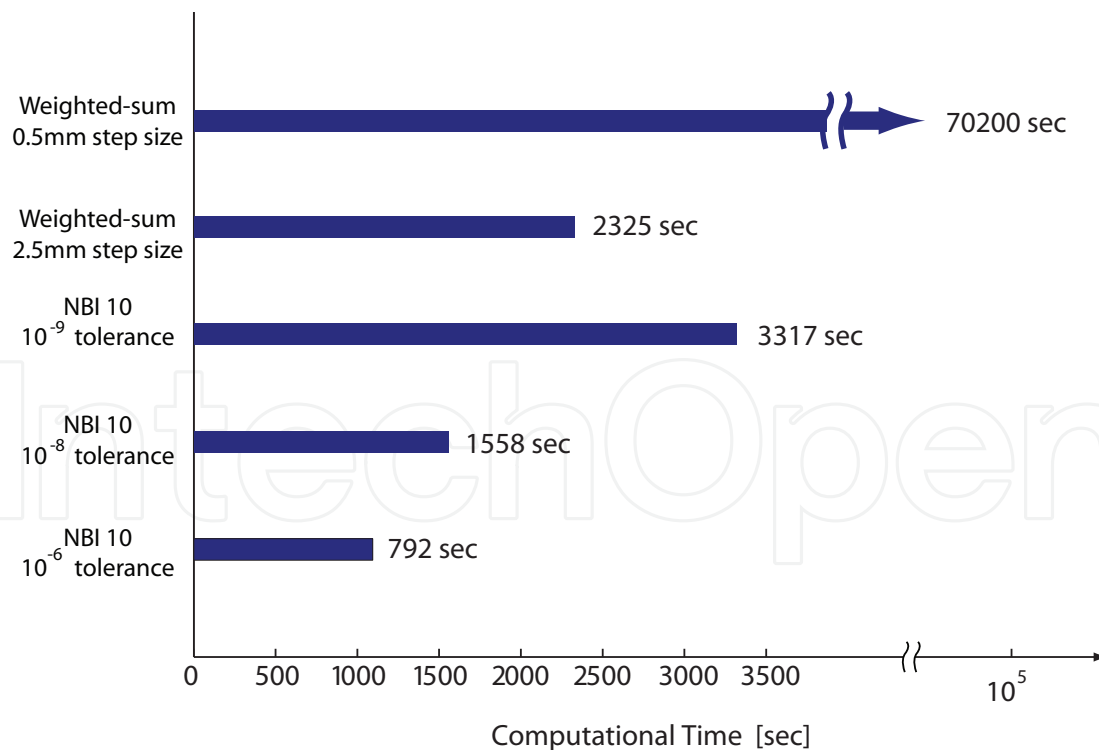


Fig. 4. Computational effort of NBI method with respect to different tolerances and weighted sum method with respect to different discretizations.

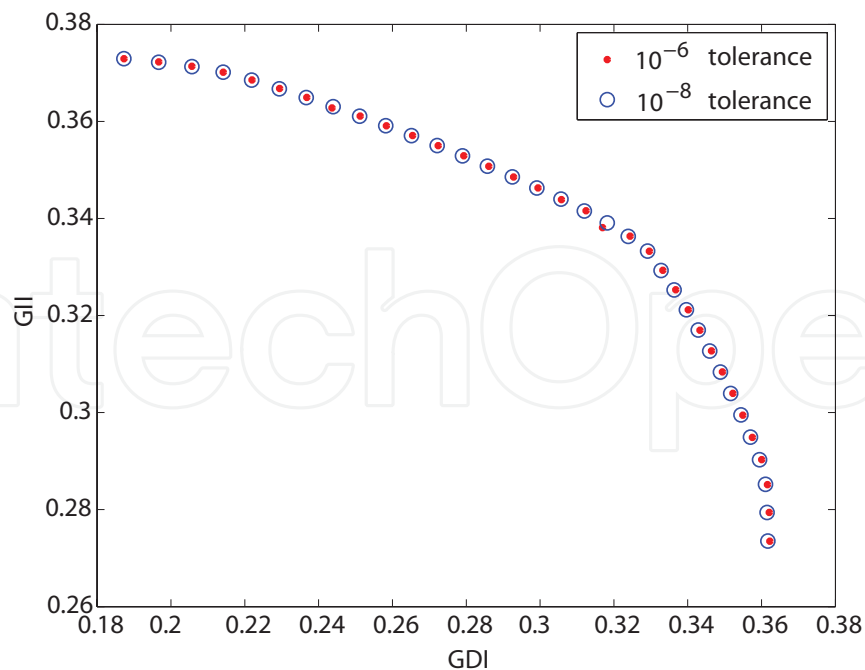


Fig. 5. Distribution of NBI solutions with two different tolerances:  $10^{-6}$  and  $10^{-8}$

acceptable in Figure 5. Since NBI employs a local search algorithm that is dependent on the initial conditions, convergence can be poor at certain trials as can be observed for a point in Figure 5. However, poor convergence of certain points is not an uncorrectable drawback, as solution for those points can be repeated with different initializations and tighter tolerances. The computational time for NBI method scales linearly with tolerance values as it does with number of points selected for the grid.

To allow for further comparisons of the Pareto methods with other scalarization approaches proposed in the literature, a sequential optimization is implemented for the sample problem as suggested in (Stocco, 1999). In this method, firstly parameter sets resulting in the best  $GII$  values for each discrete value of the parameter  $l$  are calculated using the culling algorithm. The change in  $GII$  values and the other link lengths are plotted in Figure 6 with respect to the independent parameter  $l$ . In this plot, one can observe that  $GII$  value increases monotonically with increasing  $l$  until some point, specifically at  $l = 484$ ,  $r = 583$ , after which, it becomes a monotonically decreasing function of  $l$ .

Assigning  $l$  as the independent variable, the sequential method uses the set of “optimal” solutions with respect to  $GII$  as the feasible search domain to conduct another single criteria optimization, this time with respect to  $GDI$ . In other words, the parameter set resulting in the best  $GDI$  value is selected from the Figure 6, utilizing the culling algorithm. The result of the sequential optimization approach is plotted in Figure 7 with respect to a dense Pareto-curve obtained using the NBI approach. The plot is re-scaled to have the abscissa represent the maximum singular value of the inertia matrix, which has dimensions of kg, to facilitate the selection of the final design. The process has, of course, turned the max-max problem into a min-max one, where the maximum singular value of the mass matrix over the workspace is intended to be minimized, and  $GII$  is to be maximized. As a result the Pareto curve is reflected about the vertical axis. Inspecting the plot, one can conclude that the “best” solution obtained using the sequential optimization approach is *dominated* – is a point not lying on

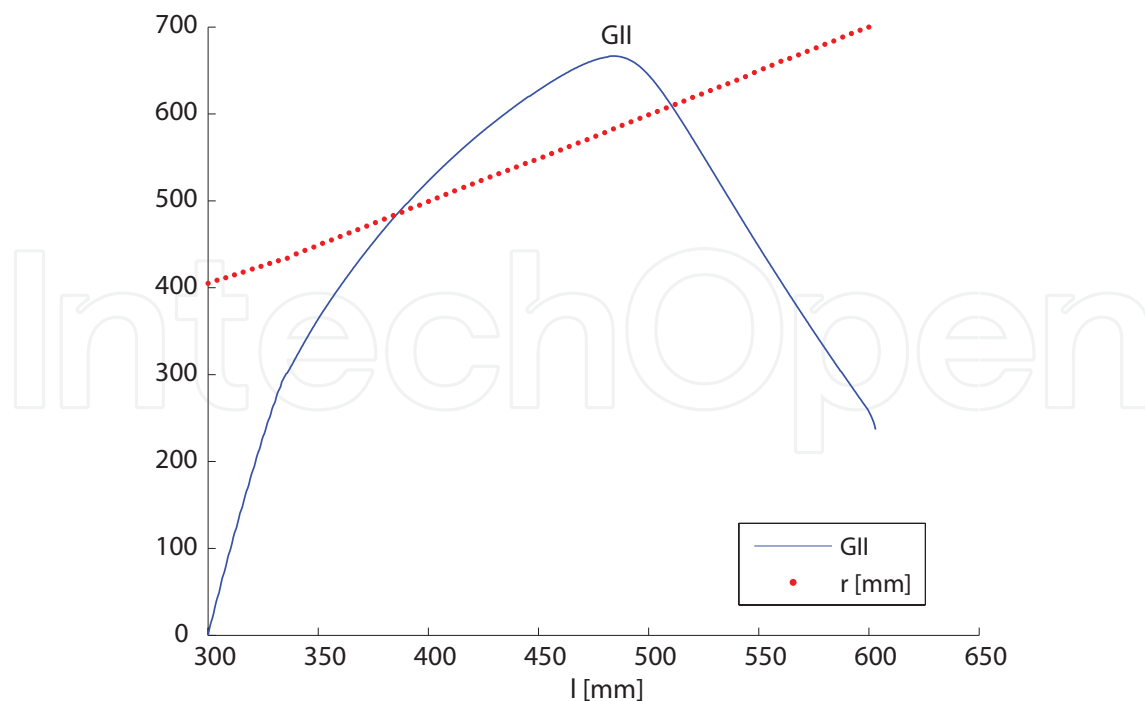


Fig. 6. The parameter sets with best  $GII$  values for each discrete value of  $l$ .

the Pareto front, meaning there exists solutions for which one can improve  $GII$  while keeping  $GDI$  constant or vice versa. In fact, improvements up to 10% in the  $GII$  value and up to 12% in the maximum singular value are possible by choosing one of the designs that lies on the Pareto-front boundary found by the intersection of the Pareto curve and vertical and horizontal line, respectively, passing through that point.

As emphasized earlier, any point on the Pareto-front curve is a non-dominated solution. Hence it is up to the designer to choose the “best” design for the application at hand, considering the characteristics of the trade-off mapped out by the Pareto-front boundary. The Pareto methods not only allow additional constraints be considered for the final decision but also let the designer adjust these constraints while simultaneously monitoring their effect on the set of non-dominated solutions. For the sample problem analyzed, a design is selected by imposing three additional physical constraints on the Pareto-front curve: a footprint constraint, a limit on the largest singular value of the mass matrix, and a threshold for the  $GII$  value. The footprint constraint of 400mm x 400mm eliminates the top 13 points of the Pareto curve. The second constraint, specifically the largest singular value of the mass matrix to be less than 250g, eliminates the 14<sup>th</sup> point in the solution set. Letting  $GII$  possess at least a value of 0.34, takes out 16 non-dominated solutions on the left. Finally, a selection is made among the remaining solutions in the set, by considering ease of manufacturing. The design is marked with a star in Figure 7. The link lengths corresponding to this design choice are  $l = 390$ mm and  $r = 470$ mm as also depicted in Figure 7.

## 7. Conclusions

A general framework suitable for optimization of haptic interfaces, in particular haptic interfaces with closed kinematic chains, with respect to multiple design criteria is presented. Optimization problems for haptic interfaces with best worst-case kinematic and dynamic per-

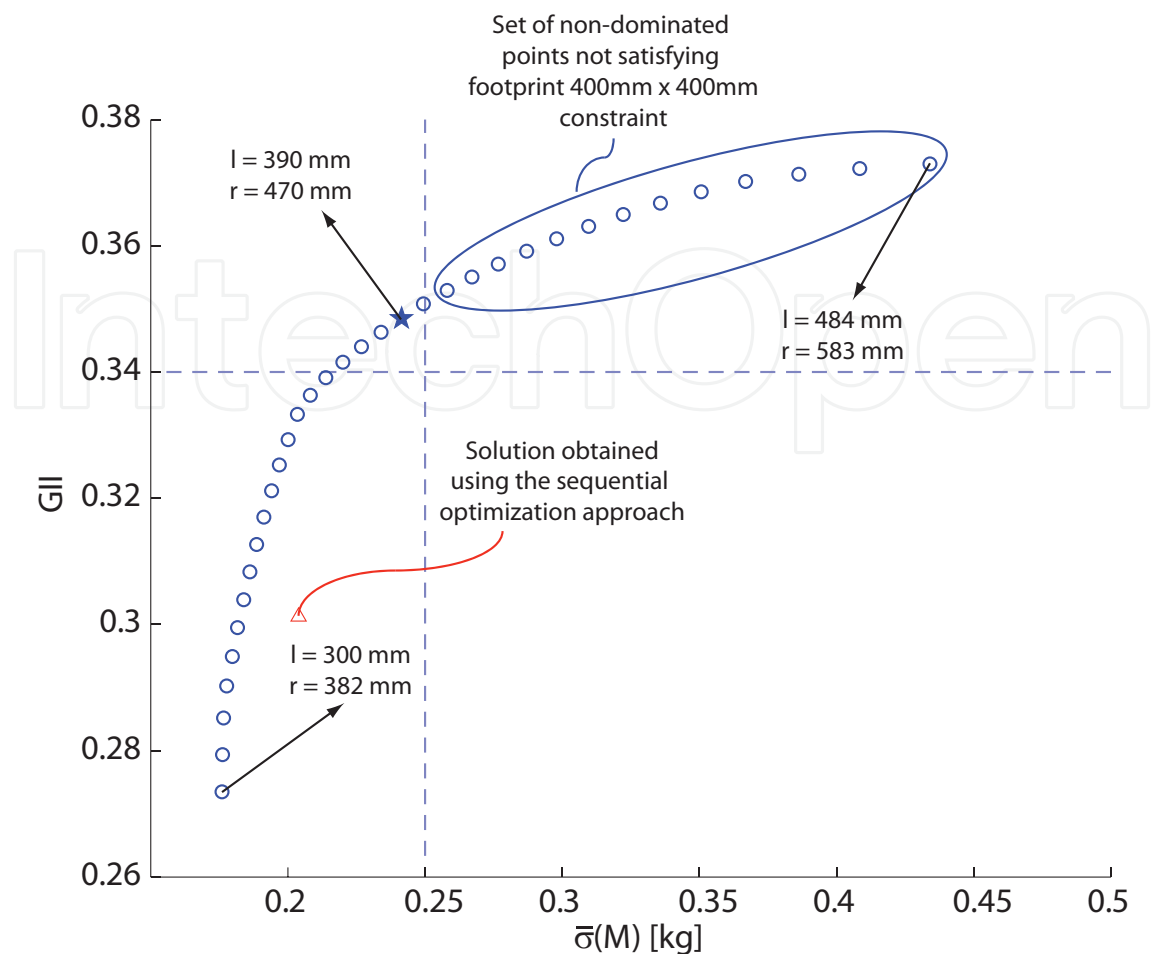


Fig. 7. Comparison of sequential approach with the Pareto-front curve. Effects of additional constraints imposed on the problem and link lengths corresponding to “best” designs.

formance are formulated. Non-convex single objective optimization problems are solved with the modified culling algorithm, while NBI method is used to obtain the Pareto-front curve to present the designer with a wide range of alternative solutions. Computational efficiency of NBI method is demonstrated over aggregating approaches such as weighted sums. The optimality of the design using Pareto methods is shown over prioritization approaches. Dimensional synthesis of a high performance haptic interface utilizing the Pareto-front curve is demonstrated.

### Acknowledgements

The authors gratefully acknowledge Gullu Kiziltas Sendur and Ramazan Unal for their valuable contributions at several stages of the framework presented.

### 8. References

Alici, G. & Shirinzadeh, B. (2004). Optimum synthesis of planar parallel manipulators based on kinematic isotropy and force balancing, *Robotica* **22**(1): 97–108.

- Asada, H. (1983). A geometrical representation of manipulator dynamics and its application to arm design, *ASME Journal of Dynamic Systems, Measurement, and Control* **105**(3): 131–135.
- Chen, W., Zhang, Q., Zhao, Z. & Gruver, W. A. (1995). Optimizing multiple performance criteria in redundant manipulators by subtask-priority control, *IEEE International Conference on Systems, Man and Cybernetics*, Vol. 3, pp. 2534–2539.
- Clavel, R. (1988). Delta: a fast robot with parallel geometry, *18th Int. Symposium on Industrial Robots, Lausanne, Switzerland*, pp. 91–100.
- Das, I. & Dennis, J. E. (1996). Normal-boundary intersection: A new method for generating the pareto surface in nonlinear multi-criteria optimization problems, *SIAM Journal on Optimization* **8**(3): 631–65.
- de Weck, O. L. (2004). Multiobjective optimization: History and promise, *China-Japan-Korea Joint Symposium on Optimization of Structural and Mechanical Systems*, Invited Keynote Paper.
- Erdogan, A., Satici, A. C. & Patoglu, V. (2009). Design of a reconfigurable force feedback ankle exoskeleton for physical therapy, *ASME/IFTOMM International Conference on Reconfigurable Mechanisms and Robots, ReMAR 2009.*, pp. 400–408.
- Fonseca, C. M. & Fleming, P. J. (1993). Genetic algorithms for multiobjective optimization: Formulation, discussion and generalization, *Multiobjective evolutionary algorithms: Empirical Genetic Algorithms*, pp. 416–423.
- Gosselin, C. & Angeles, J. (1991). A global performance index for the kinematic optimization of robotic manipulators, *ASME Journal of Mechanical Design* **113**(3): 220–226.
- Grace, K. & Colgate, J. (1993). A six degree-of freedom micromanipulator for ophthalmic surgery, *IEEE International Conference on Robotics and Automation*, Vol. 1, pp. 630–635.
- Gregorio, R. D. & Parenti-Castelli, V. (2005). On the characterization of the dynamic performances of planar manipulators, *Meccanica* **40**(3): 267–279.
- Hayward, V., Choksi, J., Lanvin, G. & Ramstein, C. (1994). Design and multi-objective optimization of a linkage for a haptic interface, *Advances in Robot Kinematics*, pp. 352–359.
- Khan, W. A. & Angeles, J. (2006). The kinetostatic optimization of robotic manipulators: The inverse and the direct problems, *Transaction of ASME Journal of Mechanical Design* **128**(1): 168–178.
- Klein, C. A. & Blaho, B. E. (1987). Dexterity measures for the design and control of kinematically redundant manipulators, *The International Journal of Robotics Research* **4**(2): 72–83.
- Krefft, M. & Hesselbach, J. (2005a). Elastodynamic optimization of parallel kinematics, *IEEE International Conference on Automation Science and Engineering*, pp. 357–362.
- Krefft, M. & Hesselbach, J. (2005b). Elastodynamic optimization of parallel kinematics, *IEEE International Conference on Automation Science and Engineering*, pp. 357–362.
- Krefft, M., Kerle, H. & Hesselbach, J. (2005). The assesment of parallel mechanisms – it is not only kinematics, *Production Engineering* **12**(1): 173–173.
- Lee, J. H., Eom, K. S., Yi, B.-J. & Suh, I. H. (2001). Design of a new 6-DoF parallel haptic device, *IEEE International Conference on Robotics and Automation*, Vol. 1, pp. 886–891.
- Lee, S.-U. & Kim, S. (2006). Analysis and optimal design of a new 6-DoF parallel type haptic device, *IEEE/RSJ International Conference on Intelligent Robots and Systems*, pp. 460–465.
- Li, Y. & Xu, Q. (2005). Dynamic analysis of a modified delta parallel robot for cardiopulmonary resuscitation, *Intelligent Robots and Systems, 2005. (IROS 2005). 2005 IEEE/RSJ International Conference on*, pp. 233–238.

- Liu, X.-J. & Wang, J. (2007). A new methodology for optimal kinematic design of parallel mechanisms, *Mechanism and Machine Theory* **42**: 1210–1224.
- Liu, X.-J., Wang, J. & Zheng, H.-J. (2006). Optimum design of the 5R symmetrical parallel manipulator with a surrounded and good-condition workspace, *Robotics and Autonomous Systems* **54**(3): 221–233.
- Lou, Y., Liu, G. & Li, Z. (2008). Randomized optimal design of parallel manipulators, *Automation Science and Engineering, IEEE Transactions on* **5**(2): 223–233.
- Ma, O. & Angeles, J. (1990). The concept of dynamic isotropy and its applications to inverse kinematics and trajectory planning, *IEEE International Conference on Robotics and Automation*, Vol. 1, pp. 481–486.
- McGhee, S., Chan, T. F., Dubey, R. V. & Kress, R. L. (1994). Probability-based weighting of performance criteria for a redundant manipulator, *ICRA*, pp. 1887–1894.
- Merlet, J.-P. (2006). Design, *Parallel Robots, 2nd Edition*, Springer, p. 303.
- Ozaki, H., Wang, H., Liu, X. & Gao, F. (1996). The atlas of the payload capability for design of 2-DoF planar parallel manipulators, *IEEE International Conference on Systems, Man, and Cybernetics*, Vol. 2, pp. 1483–1488.
- Pierrot, F., Reynaud, C. & Fournier, A. (1990). Delta: a simple and efficient parallel robot, *Robotica* **8**(2): 105–109.
- Qi, L. & Womersley, R. S. (1996). On extreme singular values of matrix valued functions, *Journal of Convex Analysis* **3**(1): 153–166.
- Rigoni, E. & Poles, S. (2005). NBI and MOGA-II, two complementary algorithms for multi-objective optimizations, *Practical Approaches to Multi-Objective Optimization*.
- Risoli, A., Prisco, G. M., Salsedo, F. & Bergamasco, M. (1999). A two degrees-of-freedom planar haptic interface with high kinematic isotropy, *IEEE International Workshop on Robot and Human Interaction*, pp. 297–302.
- Salisbury, J. K. & Craig, J. J. (1982). Articulated hands: Force control and kinematic issues, *The International Journal of Robotics Research* **1**(1): 4–17.
- Satici, A. C., Erdogan, A. & Patoglu, V. (2009). Design of a reconfigurable ankle rehabilitation robot and its use for the estimation of the ankle impedance, *IEEE International Conference on Rehabilitation Robotics, ICORR 2009*, pp. 257–264.
- Stan, S.-D., Maties, V. & Balan, R. (2006). Optimal design of 2 DoF parallel kinematics machines, *Applied Mathematics and Mechanics*, pp. 705–706.
- Stocco, L. J. (1999). *Robot design optimization with haptic interface applications*, PhD thesis, The University of British Columbia.
- Stocco, L., Salcudean, S. E. & Sassani, F. (1998). Fast constrained global minimax optimization of robot parameters, *Robotica* **16**(6): 595–605.
- Stuckman, B. & Easom, E. (1992). A comparison of bayesian/sampling global optimization techniques, *IEEE Transactions of Systems, Man and Cybernetics* **22**(5): 1024–1032.
- Stuckman, B., Evans, G. & Mollaghasemi, M. (1991). Comparison of global search methods for design optimization using simulation, *IEEE Winter Simulation Conference*, pp. 937–944.
- Tokatli, O. & Patoglu, V. (2009). Multicriteria design optimization of a compliant micro half-pantograph, *ECCOMAS Multibody Dynamics*.
- Tsai, L.-W., Walsh, G. & Stamper, R. (1996). Kinematics of a novel three dof translational platform, *Robotics and Automation, 1996. Proceedings., 1996 IEEE International Conference on*, Vol. 4, pp. 3446–3451 vol.4.

- Unal, R., Kiziltas, G. & Patoglu, V. (2008a). A multi-criteria design optimization framework for haptic interfaces, *IEEE International Symposium on Haptic interfaces for virtual environment and teleoperator systems, Haptic Symposium 2008*, pp. 231–238.
- Unal, R., Kiziltas, G. & Patoglu, V. (2008b). Multi-criteria design optimization of parallel robots, *IEEE International Conference on Cybernetics and Intelligent Systems and IEEE International Conference on Robotics, Automation and Mechatronics, CIS-RAM*.
- Unal, R. & Patoglu, V. (2008a). Optimal dimensional synthesis of a dual purpose haptic exoskeleton, *Lecture Notes in Computer Science, Springer*.
- Unal, R. & Patoglu, V. (2008b). Optimal dimensional synthesis of force feedback lower arm exoskeletons, *IEEE RAS and EMBS International Conference on Biomedical Robotics and Biomechatronics, BioRob 2008*, pp. 329–334.
- Yoon, J. & Ryu, J. (2001). Design, fabrication, and evaluation of a new haptic device using a parallel mechanism, *IEEE/ASME Transactions on Mechatronics* 6(3): 221–233.
- Yoshikawa, T. (1985a). Dynamic manipulability of robotic mechanisms, *Journal of Robotic Systems* 2(1): 113–123.
- Yoshikawa, T. (1985b). Manipulability of robotic mechanisms, *The International Journal of Robotics Research* 4(2): 3–9.
- Zheng, Y. & Lewis, W. (1994). Several algorithms of global optimal search, *Advances in Engineering Software* 22(2): 87–98.

IntechOpen



## **Advances in Haptics**

Edited by Mehrdad Hosseini Zadeh

ISBN 978-953-307-093-3

Hard cover, 722 pages

**Publisher** InTech

**Published online** 01, April, 2010

**Published in print edition** April, 2010

Haptic interfaces are divided into two main categories: force feedback and tactile. Force feedback interfaces are used to explore and modify remote/virtual objects in three physical dimensions in applications including computer-aided design, computer-assisted surgery, and computer-aided assembly. Tactile interfaces deal with surface properties such as roughness, smoothness, and temperature. Haptic research is intrinsically multi-disciplinary, incorporating computer science/engineering, control, robotics, psychophysics, and human motor control. By extending the scope of research in haptics, advances can be achieved in existing applications such as computer-aided design (CAD), tele-surgery, rehabilitation, scientific visualization, robot-assisted surgery, authentication, and graphical user interfaces (GUI), to name a few. *Advances in Haptics* presents a number of recent contributions to the field of haptics. Authors from around the world present the results of their research on various issues in the field of haptics.

### **How to reference**

In order to correctly reference this scholarly work, feel free to copy and paste the following:

Volkan Patoglu and Aykut Cihan Satici (2010). Optimal Design of Haptic Interfaces, *Advances in Haptics*, Mehrdad Hosseini Zadeh (Ed.), ISBN: 978-953-307-093-3, InTech, Available from:  
<http://www.intechopen.com/books/advances-in-haptics/optimal-design-of-haptic-interfaces>

**INTECH**  
open science | open minds

### **InTech Europe**

University Campus STeP Ri  
Slavka Krautzeka 83/A  
51000 Rijeka, Croatia  
Phone: +385 (51) 770 447  
Fax: +385 (51) 686 166  
[www.intechopen.com](http://www.intechopen.com)

### **InTech China**

Unit 405, Office Block, Hotel Equatorial Shanghai  
No.65, Yan An Road (West), Shanghai, 200040, China  
中国上海市延安西路65号上海国际贵都大饭店办公楼405单元  
Phone: +86-21-62489820  
Fax: +86-21-62489821

© 2010 The Author(s). Licensee IntechOpen. This chapter is distributed under the terms of the [Creative Commons Attribution-NonCommercial-ShareAlike-3.0 License](#), which permits use, distribution and reproduction for non-commercial purposes, provided the original is properly cited and derivative works building on this content are distributed under the same license.

IntechOpen

IntechOpen